

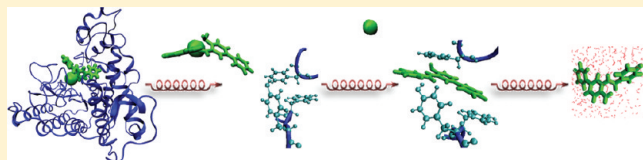
# Exploring Inhibitor Release Pathways in Histone Deacetylases Using Random Acceleration Molecular Dynamics Simulations

Subha Kalyaanamoorthy and Yi-Ping Phoebe Chen\*

Department of Computer Science and Computer Engineering, Faculty of Science, Technology and Engineering, La Trobe University, Melbourne, Australia

 Supporting Information

**ABSTRACT:** Molecular channel exploration perseveres to be the prominent solution for eliciting structure and accessibility of active site and other internal spaces of macromolecules. The volume and silhouette characterization of these channels provides answers for the issues of substrate access and ligand swapping between the obscured active site and the exterior of the protein. Histone deacetylases (HDACs) are metal-dependent enzymes that are involved in the cell growth, cell cycle regulation, and progression, and their deregulations have been linked with different types of cancers. Hence HDACs, especially the class I family, are widely recognized as the important cancer targets, and the characterizations of their structures and functions have been of special interest in cancer drug discovery. The class I HDACs are known to possess two different protein channels, an 11 Å and a 14 Å (named channels A and B1, respectively), of which the former is a ligand or substrate occupying tunnel that leads to the buried active site zinc ion and the latter is speculated to be involved in product release. In this work, we have carried out random acceleration molecular dynamics (RAMD) simulations coupled with the classical molecular dynamics to explore the release of the ligand, *N*-(2-aminophenyl) benzamide (LLX) from the active sites of the recently solved X-ray crystal structure of HDAC2 and the computationally modeled HDAC1 proteins. The RAMD simulations identified significant structural and dynamic features of the HDAC channels, especially the key ‘gate-keeping’ amino acid residues that control these channels and the ligand release events. Further, this study identified a novel and unique channel B2, a subchannel from channel B1, in the HDAC1 protein structure. The roles of water molecules in the LLX release from the HDAC1 and HDAC2 enzymes are also discussed. Such structural and dynamic properties of the HDAC protein channels that govern the ligand escape reactions will provide further mechanistic insights into the HDAC enzymes, which, in the long run, have a potential to bring new ideas for developing more promising HDAC inhibitors as well as extend our atomic level understandings on their mechanisms of action.



## INTRODUCTION

Chromatin, the fundamental unit of eukaryotic genome, is made up of DNA, histones, and nonhistone proteins. Of these, histones are chiefly involved in controlling the gene expression<sup>1</sup> via several post-translational modifications like acetylation, methylation, phosphorylation, and ubiquitination.<sup>2,3</sup> These modifications alter the electrostatic system of DNA/protein complexes, thereby creating multiple potential sites where the chromatin interacting proteins can dock. Such chromatin interactions with the proteins tend to effortlessly modify the gene expression that remains significant for malignancies.<sup>4</sup>

Acetylation and deacetylation of histones are the two central, but counteracting, epigenetic mechanisms whose balance is very crucial for the chromatin regulation of many cellular proteins.<sup>5</sup> Histone deacetylase (HDAC) enzymes modify the chromatin structures by removing the acetyl group from the  $\epsilon$ -amino lysine residues (process named as ‘deacetylation’), while the histone acetyl transferase (HAT) enzymes mediate a reverse process ‘acetylation’ by adding the acetyl group to the histone tails.<sup>6</sup> Hyperacetylation of histones leads to increased transcriptional activity, whereas the hypoacetylated histones repress the gene expression remarkably.<sup>7,8</sup> HDACs have been

reported to be involved in the alteration of gene expressions of major tumor suppressor proteins, resulting in the development of the tumor cells.<sup>6,9,10</sup> HDACs can be associated in cancers through different mechanisms like aberrant recruitment, mutations, altered level of gene expression, chromosomal translocations, etc.

Human HDAC family embraces 18 individual HDAC enzymes that are categorized into four groups based on the homology to the yeast Rpd3 deacetylase (class I), yeast Hda1 deacetylase (class II), yeast Sir2 (class III), and human HDAC11 protein (class IV). The enzyme classes, I (HDAC1–3 and 8), II (HDAC4–7, 9, and 10), and IV (HDAC11), share sequence and structural homology in their catalytic domains and also contain a zinc ion, buried into the active site, which is essential for their catalytic actions. On the other hand, the class III HDAC depends on the oxidized form of nicotinamide adenine dinucleotide ( $\text{NAD}^+$ ) for its activity.<sup>6,11–13</sup> Although class I and II HDACs are strongly associated with cancer formation, class I family has been

Received: October 3, 2011

Published: January 23, 2012



identified to play active roles in the cell proliferation.<sup>14</sup> For these reasons, there has always been special attention paid toward researching the molecular structures of the class I HDAC proteins.

Mutations or alterations in the class I HDACs generally result in the loss of their functions that in turn contribute to the cancer developments.<sup>15</sup> The tumor suppressor gene, Rb, recruits the class I HDACs to repress the gene transcription. However, the loss of activities in the class I HDAC enzymes eventually leads to the gene expressions that are regulated by the Rb gene and hence suppressing the defensive mechanisms against tumor growth.<sup>16</sup> The Uniprot database<sup>17</sup> reports experimental information on several HDAC mutations and its effect on interactions with other proteins. Ropero and Esteller have also identified a mutation in HDAC2 in sporadic tumors that showed microsatellite instability, which later lead to the loss of its activity, thus inducing the oncogene expression.<sup>18</sup> Similarly, Weerasinghe et al.<sup>12</sup> have conducted mutagenesis experiments on the nine different residues occupying the 11 Å long channel in HDAC1 structure in order to probe their influences on the catalytic activities of HDAC1 enzyme and showed that the phenylalanine residues (Phe 150 and Phe 205) present in the narrowest region of this channel are significant for the HDAC1 activities. They observed that substituting these phenylalanine residues with any other amino acids, except tyrosine, resulted in the drastic reduction of deacetylase activity of HDAC1, and while substituted with tyrosine, the deacetylase activity was reduced partially. Alongside, a number of experiments have confirmed the overexpression of HDAC1 and HDAC2 enzymes in different types of cancers.<sup>19,20</sup>

The catalytic mechanism of the zinc-dependent HDACs is described well in the literature.<sup>21–23</sup> HDACs generally operate within large multiprotein complexes interacting with a number of other proteins like NCoR, Sin3, NuRD, and CoREST and remove the acetyl groups from the lysine residues of the target proteins. The removal of the acetyl group occurs via a charge relay system (also known as 'His-Asp' charge relay system) that involves two adjacent histidine residues, two aspartate residues, and one tyrosine residue. The divalent zinc ion that is buried into the active site of HDACs is essential for the 'His-Asp' charge relay system<sup>22</sup> and thus the functionality of the HDACs. The zinc ion in the catalytic center of the HDAC polarizes the carbonyl group of the acetate product, thereby increasing the electrophilicity of its carbonyl carbon.<sup>21</sup> Further, the zinc ion coordinates with a catalytic water molecule which is hydrogen bonded to a pair of histidine residues that further make hydrogen bonds with the aspartate residues, completing the 'His-Asp' charge relay system. Moreover, the active site water molecule is close to the carbonyl carbon of the lysine substrate and hence leads to a nucleophilic attack on the carbonyl carbon. The hydroxyl moiety of a tyrosine residue which is present close to the zinc ion, but opposite to the charge relay system in the active site, forms a hydrogen bond with the substrate's carbonyl oxygen and protonates the amino group of the reaction product.

Inhibitions of these HDACs have shown to induce terminal differentiation, growth arrest, and apoptosis in a number of cancerous cells and thus remain a promising target for cancer therapy.<sup>24,25</sup> An HDAC inhibitor (HDACi) is generally composed of a zinc binding group (ZBG) to chelate the catalytic ion, a capping region to occupy the opening of the active site cavity, and a linker that links the ZBG and the cap. Any HDACi with its strong ZBG is able to inhibit the HDACs

by replacing the substrate and preserving the 'His-Asp' charge-transfer system within the enzyme complex. A variety of inhibition mechanisms by these HDACi's are discussed elsewhere.<sup>26,27</sup> Following decades of consistent works, researchers have already identified a number of potential classes of HDACi that include two recent FDA-approved drugs, suberoylanilide hydroxamic acid (SAHA) and FK228,<sup>28</sup> while some of them are in preclinical and clinical trials.<sup>1,29,30</sup> Yet, until today, there have been lots of draw backs in the attempt of discovering one promising anticancer compound specific to each of the HDAC family proteins. When researchers have put in momentous efforts in searching possible inhibitors against HDACs, much information on the enzymes themselves are not yet revealed.

Channels or pathways are one of the decisive features of the proteins that can help in understanding the relationships between the structures and activities of various chemical entities. More particularly in enzymes like HDACs, where the active site is buried, these proteins channels can be useful in accessing/dissociating from the catalytic sites. Hence, the size and shape of these channels and cavities play a vital role in the catalytic activity and specificity of the proteins.<sup>31</sup> HDACs and HDAC-like protein (HDLP) were found to possess a tubelike, 11 Å long channel,<sup>12</sup> which extends to the active site and accommodates the zinc ion at the bottom of this channel. We represent this channel as 'channel A' and is built up of seven loops<sup>32,33</sup> that are primarily composed of aromatic amino acid residues. The walls of the pocket are mostly covered with the hydrophobic amino acid residues, and two phenyl groups facing opposite to each other mark the most slender portion of this channel.<sup>23</sup> Further, adjacent to the zinc ion, another 14 Å long internal cavity (or foot pocket) is realized in the HDLP<sup>33,34</sup> and in the crystal structures of HDAC2<sup>35</sup> and HDAC8.<sup>21,36</sup> We name this channel as 'channel B1' in this work. This water-filled foot pocket was hypothesized as the evacuation route for the acetate byproduct.<sup>12,21,23,33,35,37</sup> To check this hypothesis, very recently, Whitehead et al.<sup>38</sup> docked the acetic acid into the 14 Å long internal cavity of HDLP protein and identified that the acetic acid settled well into this internal cavity by making hydrogen bonding with Ile-19 and Trp-137 residues. Further, Wang et al.<sup>33,37</sup> docked nine different HDAC1 inhibitors into the HDLPs structure and identified that this 14 Å cavity can serve as a second binding pocket for the additional interactions of HDACi. However, such studies on the 14 Å cavities of the class I HDAC enzymes, except HDAC8,<sup>21,36</sup> are rather scarce. Moreover, the unbinding of ligand from the HDAC enzymes through this channel or via channel A and the gate residues involving in the opening and closing of these channels has not been reported yet.

Given the importance of the protein channels and ligand dissociation through these channels, a number of approaches have been used to study the unbinding mechanisms, such as dynamic map ensemble approach,<sup>39</sup> metadynamics,<sup>40,41</sup> steered molecular dynamics (SMD),<sup>42,43</sup> random acceleration molecular dynamics (RAMD), etc.<sup>44</sup> Of these, RAMD and SMD have gained popularity for studying the ligand release protein channels. Compared to the other approaches, SMD offers a more detailed mapping of the energy and the force profiles along the given direction of the pathway. Hence, SMD requires predefined pathway information to simulate ligand release. On the other hand, RAMD does not require predefinitions of pathway directions to predict the ligand exit. With a small optimum force and threshold distance parameters, the RAMD

approach allows the ligand to search the possible egress pathways in an unbiased nature and within reasonable time scales. Ligand egressions from different enzymes, such as haloalkane dehalogenase,<sup>45,46</sup> human cytochrome P450 enzymes,<sup>47</sup> liver fatty acid binding protein,<sup>48</sup>  $\beta_2$ -adrenergic receptor,<sup>49</sup> opsin,<sup>50</sup> etc., have been successfully simulated and reported.

Hence, in this work, we explore the ligand unbinding mechanisms of the recently recorded crystallographic structure of HDAC2 [PDB ID: 3MAX]<sup>35</sup> and the computationally modeled HDAC1 proteins to ascertain their possible ligand release pathways through RAMD simulations.<sup>44</sup> The crystal structure of the HDAC2 protein was recently solved by Bressi et al.<sup>35</sup> with an *N*-(2-aminophenyl) benzamide (LLX), a benzamide inhibitor, bound into the active site through channel A and also extending into the foot pocket or the channel B1. LLX has been found to show different inhibition against the HDAC1 and HDAC2 enzymes. For example, Bressi and his group,<sup>35</sup> in their recent work, showed that LLX possesses a IC<sub>50</sub> value of 27 nm against HDAC2, while the chemEMBLdb database<sup>51</sup> reports a IC<sub>50</sub> value of 60 nm against the HDAC1 enzyme. At the same time, there are already a few benzamide derivatives that have been identified to show considerable efficiencies against HDAC enzymes.<sup>52–54</sup> And hence, studying the unbinding mechanism of LLX from the HDAC1 and HDAC2 enzymes could be useful to understand the dissociation mechanisms of benzamide based HDACi's, from the buried active site, besides providing insights into the target structures. However, the experimental structure of HDAC1 is not available yet, and hence, we use the homology modeled structure of HDAC1.

In this study, we investigated the known pathways and also identified additional pathways for ligand release and water exchange in HDAC1 and HDAC2 enzymes. We located and characterized the key amino acid residues that control the protein channels and also unraveled the role of water molecules in the ligand unbinding mechanisms from the HDAC1 and HDAC2 enzymes. Hence, the ligand unbinding RAMD simulations presented here are not only useful to understand the protein channels of HDAC enzymes but also the key structural and dynamic changes that take place within the enzymes during ligand dissociation. Such information provides novel mechanistic insights into the HDAC enzymes and the inhibitors.

## METHODOLOGY

**Initial Model Building.** The recently solved crystal structure of the human HDAC2 protein (PDB ID: 3MAX)<sup>35</sup> was retrieved from the Protein Data Bank (PDB) and used in this work. The experimental structure of HDAC1 is not yet available, thus the homology-based molecular modeling technique was used for constructing its three-dimensional (3D) structure. Until recently, the HDLP protein and HDAC8 protein structures were used to model HDAC1 enzyme as they had more sequence identities, such as 35.2% with HDLP and 43% with HDAC8.<sup>55</sup> However, HDAC2, whose experimental structure is currently available, has 91% of identity against HDAC1 (Figure 1, Supporting Information). Hence, the structure of HDAC2 was used as a template to model the 3D structure of human HDAC1. The amino acid (AA) sequences of the human HDAC1 with 482 AA residues (Swiss Prot ID: Q13547) was downloaded from the Swiss-Prot protein sequence database [[www.expasy.ch/sprot/](http://www.expasy.ch/sprot/)]. A BLAST search,

with BLOSUM62 substitution matrix, identified the human HDAC2 (3MAX) of 2.05 Å resolution, as suitable template structure. While modeling HDAC1, the penta-coordinated zinc metal ions and the ligand, LLX, were extracted from the HDAC2 structure to acquire the penta-coordinated geometry of the catalytic zinc metal ion. Further, the HDAC1 structure was modeled with a nonbonded zinc method that includes the van der Waals and electrostatic terms. This nonbonded method has been identified to be appropriate for the divalent zinc ion and also a few other divalent metal ions, such as Ca<sup>2+</sup>, Mg<sup>2+</sup> and Cd<sup>2+</sup>, which have closed shells.<sup>56</sup> Stote and Karplus have shown that this nonbonded model can be used for the simulations involving zinc binding sites in proteins and solution.<sup>56</sup> Further, Weerasinghe et al.<sup>12</sup> have also implied the nonbonded zinc method in their combined molecular dynamics (MD) and experimental studies on the HDAC1 structures. Hence, we used this nonbonded method so as to observe the changes in the geometry and the coordination around the zinc ion, over simulation time.

The modeled structures were further refined by correcting the missing side chain atoms, assigning the bond orders and adding the polar hydrogen atoms to the receptors. Finally, the receptor structures were minimized using OPLS2001 force field<sup>57</sup> to obtain the stable structures. Superimposition of the modeled and the template structures displayed variations only in the loop regions, which are the more flexible elements in the HDAC family, but still their root-mean-square deviation (RMSD) were well below 1 Å (Figure 2, Supporting Information). The Ramachandran plot analyses confirmed the quality of the modeled 3D structure of HDAC1 (Figure 3, Supporting Information). Hence, the 3D structures of the HDAC enzymes were made available after multiple iterations of careful refinements. Prime module of the ‘state-of-the-art’ Schrodinger drug discovery package<sup>58,59</sup> was employed in all the above steps of modeling and structure refinement. Thus, good quality 3D structures of the HDAC1 and HDAC2 proteins were used in this MD-based investigation.

**MD Simulations.** Proteins, being vibrant biomolecules, often change their conformations to stabilize themselves from an ensemble of structural arrangements. Sampling of such dynamic conformations through an effective MD protocol has been a research interest for a long time. Proteins generally exhibit increased active conformation sampling when bound to small molecule ligands compared to their native, ‘ligand-free’ state.<sup>60</sup> Water being the universal solvent medium of cells endorses various conformational changes in proteins.<sup>61</sup> This solvent flux directs the reallocation of the flexible structural segments of the protein, thereby paving the substrate/ligand binding and unbinding mechanism through protein matrix or permanent/transient tunnels. Further, these ligands have the ability to induce conformational changes to facilitate their movement through the protein matrix, whereas the tunnel access is powered by protein motions, water flux, and bonded/nonbonded interactions.<sup>62–64</sup> Thus, in order to explore the ligand-induced changes within the HDAC1 and HDAC2 proteins, we have initially carried out the classical MD simulations of the solvated proteins in their ligand-bound and -free states.

**Simulation Parameters.** All the MD simulations were carried out with the CHARMM22 force field<sup>65</sup> parameters embedded in the NAMD 2.7b3 package.<sup>66</sup> The ligand LLX in this study was parametrized using the Swissparam server<sup>67</sup> that helps in generating the force field parameters of small organic

Table 1. Backbone RMSD of HDAC1 and HDAC2 MD Simulations<sup>a</sup>

target	backbone RMSD from the initial frame (Å)		noh RMSD from the initial frame (Å)		trace RMSD from the initial frame (Å)		duration of simulation (ns)
	RMSD	SD	RMSD	SD	RMSD	SD	
HDAC1 (without ligand)	0.83	0.089	1.27	0.135	0.86	0.094	5
HDAC1 (with ligand)	1.03	0.097	1.47	0.144	1.06	0.099	5
HDAC2 (without ligand)	0.92	0.144	1.33	0.188	0.94	0.149	5
HDAC2 (with ligand)	0.98	0.156	1.37	0.165	0.99	0.159	5

<sup>a</sup>SD is standard deviations (over all); noh is all nonhydrogen heavy atoms; and trace is C<sub>α</sub> atoms.

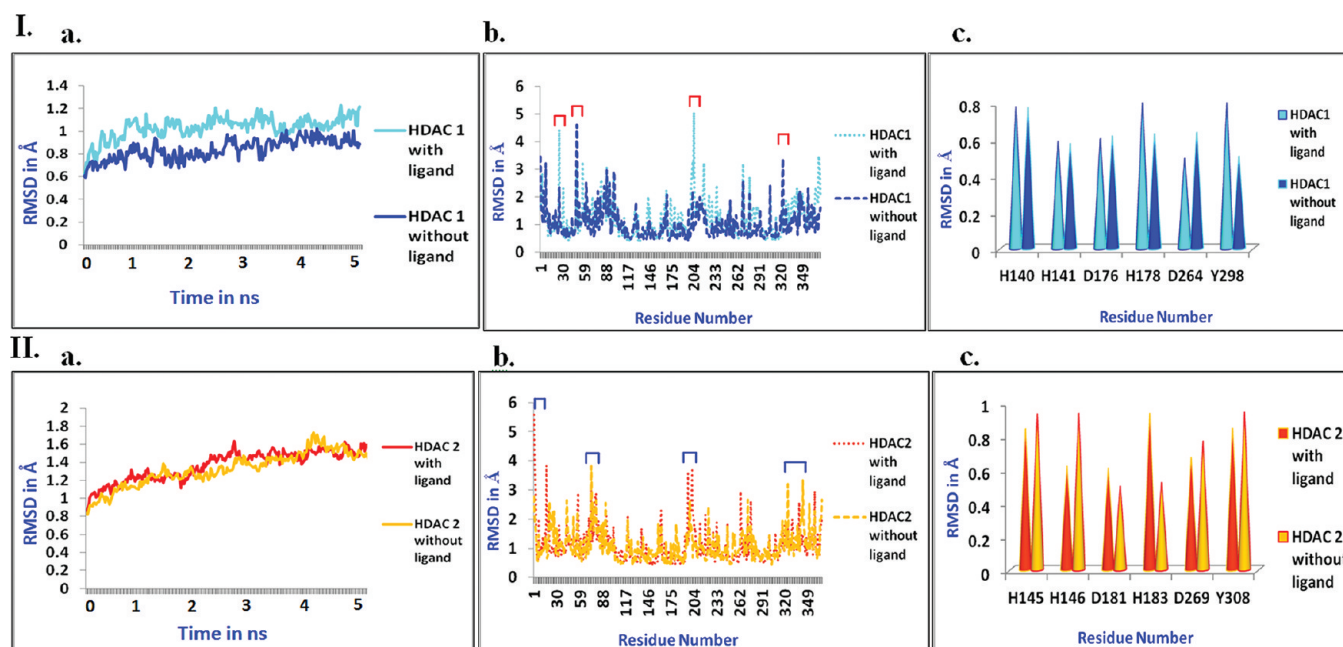


**Figure 1.** Backbone RMSD graphs of HDACs' MD simulations with respect to the initial frame of the trajectories. (a) Comparative backbone RMSDs of HDAC1 (I) and HDAC2 (II) structures with ligand-free and -bond states. (a) The per residue backbone RMSDs of HDAC1 (I) and HDAC2 (II) proteins with and without ligand. Residues that have greater than 2.5 Å RMSD are marked in bracket lines. (c) Active site backbone RMSDs of HDAC1 (I) and HDAC2 (II) proteins with and without ligand.

molecules. The Merck molecular field (MMFF)<sup>68</sup> atom types were identified using the input mol2 file from which a protein structure file (psf) for the ligand was generated. The internal coordinates (IC) of the molecule were acquired from the psf file and translated into CHARMM system unit. The residue topology and parameter file were generated from the CHARMM system unit.

MD simulations were performed on the ligand-bound and -free systems of HDAC1 and HDAC2 enzymes. These four different initial structures were solvated with TIP3P waters and electroneutralized by adding 0.15 mol/L of sodium chloride ions before minimization. Periodic boundary conditions were applied, and the particle mesh Ewald method<sup>69</sup> was used to calculate the long-range electrostatic interactions of every time steps. All classical MD simulations were carried out for 5 ns at 300 K temperature and 1 atm pressure maintained by the Langevin piston method.<sup>70</sup> Detailed simulation parameters can be found in Supporting Information.

**RAMD.** Besides inducing the desired biological response, the ligands are released to reinstate the free protein for binding another ligand. Further, the binding and release events have the propensity to throw in the details of ligand–protein interactions for any novel drug discovery effort.<sup>71</sup> The RAMD approach has been effectively used in revealing the ligand unbinding pathways for many biologically interesting

macromolecules.<sup>37,42,45,72–75</sup> This involves an even-handed exploration of the possible ligand unbinding pathways by applying a small randomly oriented force to the center of mass of the ligand besides the usual force field. During this application, the ligand tends to travel around the binding site and chooses its own direction to expel out of the protein, at a feasible time frame. The random force is generally applied for a constant time step  $N$ , with a constant force magnitude  $F$  to accelerate the ligand out of the binding pocket. The direction of acceleration is determined by a random seed generator. When there is a barrier at a particular route, the ligand chooses a new direction for the pulling force in order to cover the threshold distance,  $r_{\min}$  within the  $N$  time steps of simulation.

Five snapshots were taken from the last 200 ps of the well-equilibrated HDAC systems and were used as the initial structures for RAMD simulations. Several combinations of parameters were tested for finding the expulsion pathway. Acceleration and threshold distances are the most important parameters for the RAMD simulations, and hence, these parameters must be carefully selected. Inappropriate acceleration may result in larger conformational changes and consequently lead to non-natural ligand exit routes. The acceleration and threshold distance values of 0.04/0.05 kcal/Å/g and 0.002/0.004 Å for haloalkane dehalogenase<sup>45,46</sup> and 0.14/0.20 kcal/Å/g and 0.005/0.01 Å for human cytochrome P450

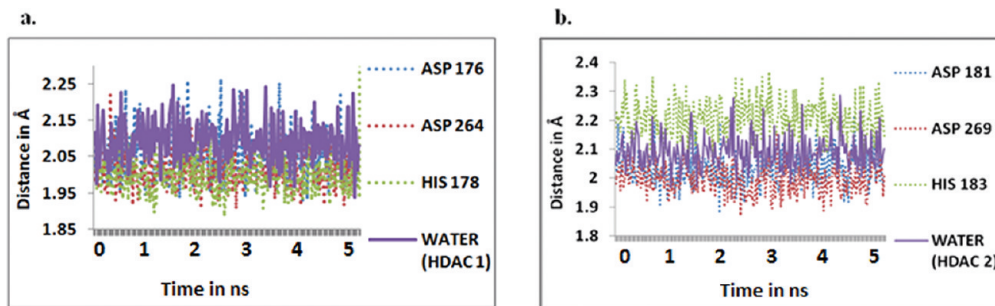


**Figure 2.** Water coordination in ligand-free systems. Distance between zinc metal and its coordinating molecules within the ligand-free HDAC1 (a) and HDAC2 (b) proteins.

enzyme<sup>47</sup> were sufficient to observe reliable exit mechanisms. However, the acceleration values of 0.35/0.40 kcal/Å/g and threshold distances of 0.002/0.008 Å were found appropriate to evidence ligand exits from the HDAC1 and HDAC2 enzymes, within feasible time frames, and hence were chosen for this study. All four combinations of chosen acceleration and threshold distance were used to simulate each of the five input structures for duration of 1 ns that employed the alternating 40 steps of RAMD and 20 steps of classical MD protocol. Hence, a total of 40 egress trajectories, 20 for each HDAC structure, were obtained and analyzed.

The conformational changes in the gate residues identified from the RAMD simulations were described as the polar graphs generated using the matrix laboratory, MATLAB R2009b numerical computing program.<sup>76</sup> The polar plot shows the distribution of the angular coordinate along the length of the trajectory. Detailed information about the polar plots can be found from the MathWorks documentation at <http://www.mathworks.com.au/help/techdoc/ref/polar.html>.

## RESULTS

**MD Simulations: Structural Stabilities.** The four different molecular systems of the HDAC1 and HDAC2 enzymes (two ligand-bound and two ligand-free configurations) under the isothermal–isobaric NPT ensemble-based classical MD simulations had stabilized very well. All the essential parameters, temperature, pressure, and total energies, converged at the end of the simulations. Following the successful simulations, the MD trajectories of all the models were investigated for the conformational space and the dynamical behaviors of the HDACs. The averaged backbone RMSDs and their standard deviations of ligand-bound and -free states of HDAC1 and HDAC2 enzymes are given (Table 1). The averaged RMSDs of the ligand-bound HDAC1 and HDAC2 were 1.03 and 0.98 Å, respectively, whereas the averaged backbone RMSDs of the ligand-free HDAC1 and HDAC2 proteins were 0.83 and 0.92 Å (Figure 1, Ia and IIa). These explained that both the bound and unbound systems evolved with very similar RMSDs, especially in HDAC2 systems. But, in HDAC1, the change was slightly larger than HDAC2. As mentioned in the Initial Model Building Section, the loop regions displayed variations when aligned with the HDAC2 template, which exhibited greater flexibility in also the MD simulations. These can be observed in the per residue RMSD plots of the ligand-bound and -unbound HDAC systems (Figure 1, Ia and IIa), where the residues constituted in the loop regions of the proteins showed higher RMSDs that were above 2.0 Å (regions marked in the figures), while the RMSDs of the rest of the residues were below 2.0 Å. Especially, the

residual ranges, 201–220 in HDAC1 and 190–210 in HDAC2, exhibited larger RMSDs. Hence, the loops around the active site and the terminal regions were more flexible and were prone to accommodate any dynamical activities taking place within the proteins. The Protein Structural Change Database (PSCD),<sup>77</sup> a database representing the relationship between protein structural changes upon ligand binding, showed that the RMSD of the ligand-bound form of the HDLP protein was only 1 Å. Such information for the HDAC crystal structure was not available in the database. However, the RMSD of ligand-bound HDLP enzyme was close to our simulations. Thus, it can be inferred that the RMSDs of the MD simulations are statistically trivial, and the overall structures of the ligand-bound and -free systems were similar and stable.

In HDACs, three amino acid residues (one HIS178/183 and two ASP176,264/ASP181,269) contributed to the first catalytic sphere (residues within the first coordination shell of the zinc ion), whereas, two HIS140,141/HIS145,146, two Tyr204,298/Tyr209,308, one GLY149/154, and one ASP99/104 constituted the second catalytic sphere. The behaviors of these amino acid residues over simulation were essential for understanding the biological roles of the HDAC proteins. In the MDs, these residues were very stable throughout the simulations, with their RMSDs ranging between 0.6 and 0.9 Å in HDAC1 and 0.4–1.1 Å in HDAC2 (Figure 1, Ic and IIc). These revealed that the active site residues of both the HDAC proteins were structurally conserved and did not undergo much side chain and backbone conformational changes.

**Zinc Coordination.** The active site zinc coordination is one of the vital structural features of the HDAC enzymes essential for their catalytic actions. First, in the ligand-free HDAC systems, the active site zinc metal ion maintained tetra-coordination with the protein environment via three amino acid residues (HIS178/183 and ASP176,264/ASP181,269) and one water molecule throughout the simulations in both HDAC1 and HDAC2 (Figure 2). Thus, zinc was ready to bond with the substrate/ligand to achieve the actual penta-coordination. In addition, two other oxygen atoms from two ASP(176,264/181,269) residues were found to be in the proximity of the zinc ion.

The X-ray crystal structure of HDAC2 protein possessed penta-coordinated zinc metal binding site which was bound with the LLX. However, the HDAC1 structure was modeled with the nonbonded zinc method so as to observe the geometry and the coordination around the zinc ion over simulation time. Thus at the end of the classical simulations, the zinc metal ion in these ligand-bound complexes displayed the expected penta-coordination.

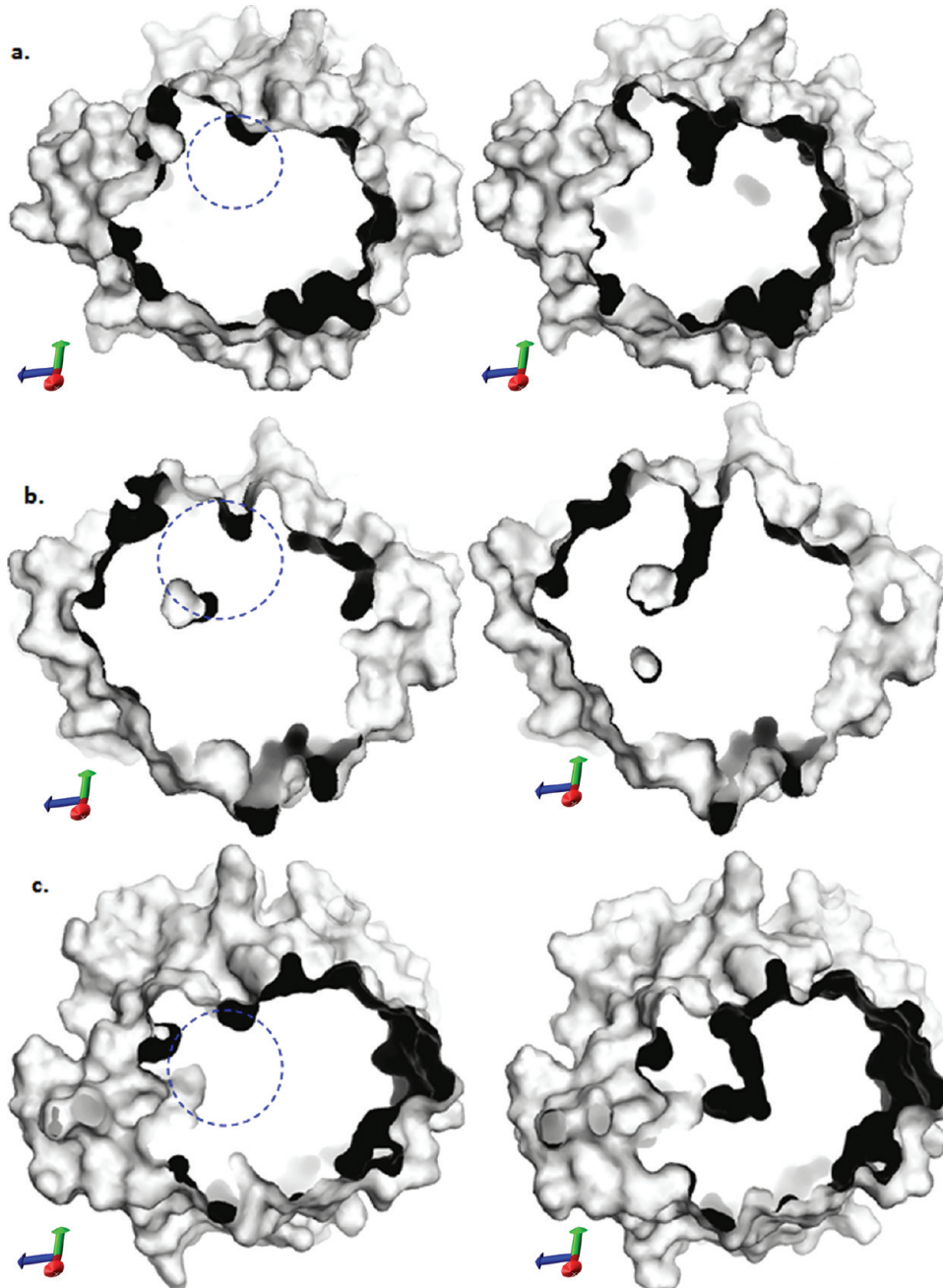


**Figure 3.** Snapshots showing the open and closed channels in HDAC1 MD simulations. Slice through surface representation of the HDAC1 enzyme showing (a) closed and open channel A, (b) closed and open channel B1, and (c) closed and open channel B2.

**Water Exchange in Classical MD Simulations.** Classical MD simulations revealed information on the active site residues HIS178/183, HIS140,141/HIS145, 146, ASP176, 264/ASP181, 269, ASP99/104, Tyr204, Tyr298/209, 308, and GLY149/154 and the ligand binding into the active site of the HDACs. In addition to this binding site information, water exchange between the active site and the bulk solvents was observed to take place via different channels in the ligand-bound and -free structures of HDAC enzymes. In the ligand-free states, the water molecules traversed through both channels A and B1 in the HDAC1 and HDAC2 enzymes (Figure 4a, Supporting Information). However, in HDAC1, water molecules were also found to exchange via a subchannel of channel B1 (Figure 4b, Supporting Information). We name this channel as ‘channel B2’

in this work. In contrast to the ligand-free states, the water exchange in the ligand-bound structures of the HDAC1 and HDAC2 enzymes took place only via channel B1 (in both HDAC1 and HDAC2) and channel B2 (in HDAC1 only) but not through channel A, as the ligand, LLX, mostly occupied this channel and hence blocked this path for water exchange into the buried active site (Figure 4c, Supporting Information). In addition to these channels, water molecules also accessed the binding site via two other narrow channels that were close to the direction of channels A and B2 in both the LLX-bound and -free HDAC structures. Moreover all the channels, A, B1, and B2, were found to open and close over the 5 ns of MD simulations. A slice through surface representations showed the open and closed states of all the channels in the HDAC1

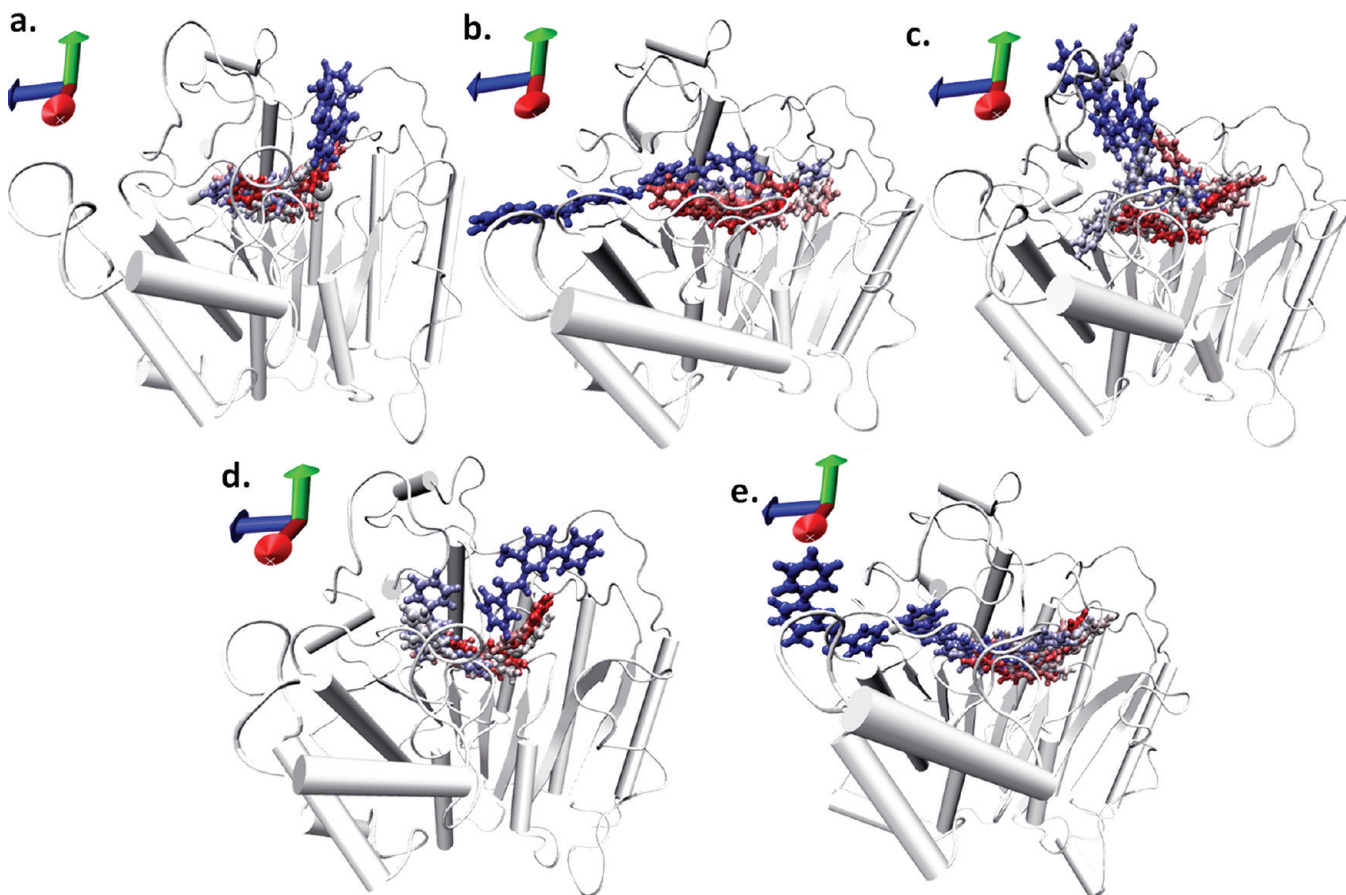


**Figure 4.** The ligand egress trajectories of HDAC1 and HDAC2, showing the direction of ligand exit. (a–c) Channels A, B1, and B2 of HDAC1 and (d,e) channels A and B of HDAC2. Red and blue coloring of the ligand refers to the initial and the final frame.

(Figure 3) and HDAC2 (Figure 5, Supporting Information). However, ligand expulsions were not witnessed in both the HDAC1 and HDAC2 in the course of classical MD simulations. Due to the very strong electrostatic interactions among the LLX, the divalent zinc ion, and the other active site residues mentioned above, classical MD simulations were not sufficient to observe the ligand release event, and hence, force-based RAMD simulations become inevitable.

**Exploration of Ligand Exit Pathways.** Since the ligand expulsions were not witnessed in the classical MD simulations of the HDAC1 and HDAC2 enzymes, RAMD simulations were performed with the combinations of chosen acceleration 0.35 and 0.40 kcal/Å/g and threshold distances of 0.002 and 0.008 Å on the five input different structures of the HDAC1 and HDAC2 proteins that were chosen from their classical MD simulations. Forty steps of RAMD simulations and 20 steps of classical MD simulations were carried out alternately.

Investigations on the RAMD trajectories revealed the unbinding of the ligand through different pathways in the target structures. The computationally modeled HDAC1 structure witnessed ligand egression through three different pathways, channels A, B1, and B2 (Figure 4a–c, respectively), identified among which 35% of egress trajectories were via channel A, another 30% via channel B1, and the rest 30% through channel B2. In 5% of the trajectories, the ligand did not end up in egression. However, in the X-ray crystallographic structure of HDAC2, there was only two pathways channels A and B1 (Figure 4d,e). Out of 20 egress trajectories in HDAC2, 10 egresses were through channel A and 9 through channel B1

and one did not witness ligand expulsion within the 1 ns time frame. High expulsion rates of similar scale were also previously reported in the REMD and RAMD investigations of liver fatty acid binding protein<sup>48</sup> and  $\beta_2$ -adrenergic receptors.<sup>49</sup> The former observed 92.14% of successful expulsions and the latter had been reported with 95% of egression rate.

Channels A and B1 were almost identical in both the HDACs, while channel B2 was found to be present only in HDAC1 protein from our 20 sampled trajectories. The characteristics of these protein channels, the key residues assisting the ligand unbinding mechanisms, and the significant water exchange between the active site and the bulk water are discussed in the following sections.

**Characteristics of Channel A.** Since the active site residues in HDAC1 and HDAC2 were highly conserved, this channel, which was close to the active sites, was also structurally similar. When a small force was applied to the ligand, LLX, it first destabilized the interactions between the ligand and the zinc ion that eventually broke the coordination interaction between them. Further, due to the strong hydrophobic contact between the ligand's linker region and the two phenylalanine residues (Phe 150 and Phe 205 in HDAC1; Phe 155 and Phe 210 in HDAC2) that were located parallel to each other in the second sphere of the catalytic zinc ion, the ligand was inside the active site for a short span. But gradually, the ligand was released from its first hydrophobic contact with Phe 205 in HDAC1 and Phe 210 in HDAC2. However, the ligand was still found to be inside the pocket of the catalytic site waiting for the 'green' signal from the other Phe residue (Phe 150 in HDAC1

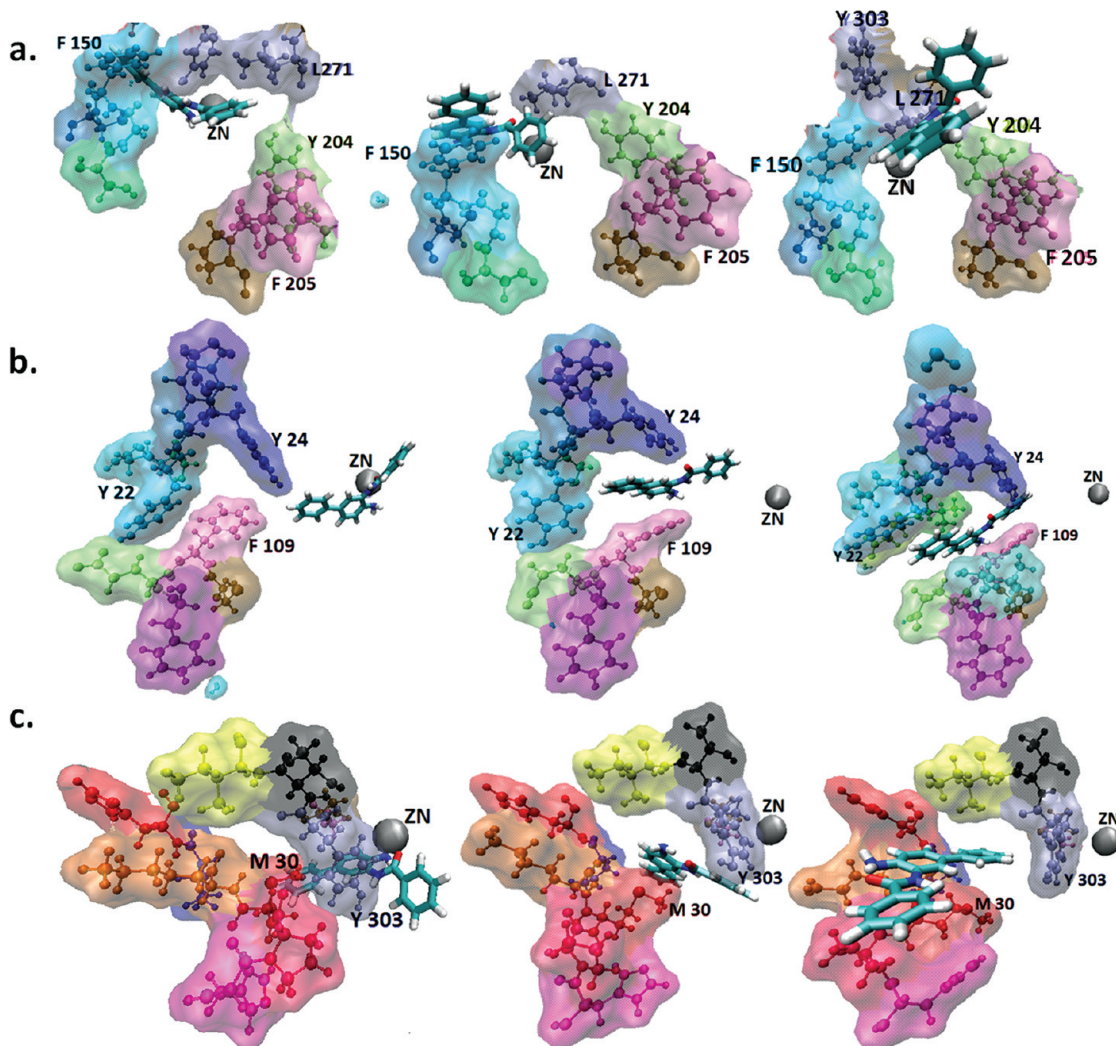


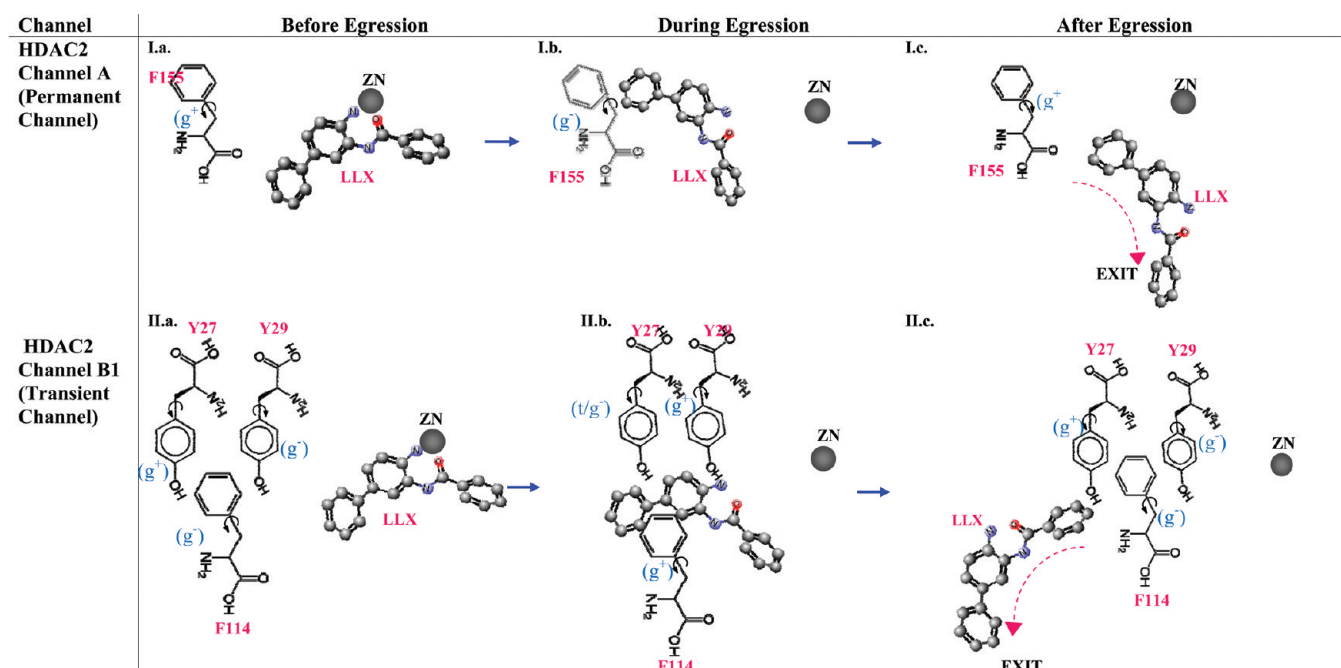
**Figure 5.** Ligand unbinding mechanisms through different channels of HDAC1. (a–c) Channels A, B1, and B2. The residues and their structural changes involving in the gating processes of all the protein channels in HDAC1 are displayed.

and Phe 155 in HDAC2) which outlined the narrow channel A. Ultimately, this Phe residue tilted its phenyl ring in the direction away from the zinc ion, thereby giving more room for the ligand to exit via the channel A (Figure 5a and Table 2). In addition to the Phe residue's rotation, few water molecules passed through the channel, thereby disrupting the interactions between the residues lining this channel and widening the passage for the ligand to move freely (Figure 6a). And this time, the LLX drew further back into the catalytic site and quickly moved forward toward the exit, mimicking the operation of a battle-field 'cannon'. Once the ligand crossed the Phe residue, it effortlessly exited the proteins. This indicated that the Phe 150/155 residue in HDAC1/2 remained a vital element in controlling the ligand release. This was also evidenced from a short time change in the dihedral angle of the Phe 150/155 residue (Table 3). Moreover, the dihedral angle of Phe 150/155 was close to  $-60^\circ$  throughout the simulation, except a few frames when it shifted to absolute  $180^\circ$  and  $60^\circ$  and returned back to the  $-60^\circ$  at the end of the simulation (Table 3). Thus, it was inferred that the aromatic heads of the Phe 150/155 residue drifted itself from the gauche<sup>−</sup> to gauche<sup>+</sup> conformation to allow the ligand to pass through it toward the exit. Interestingly, when the ligand exited the catalytic site, the water molecules moved toward the catalytic center and substituted

the LLX in maintaining the coordination of the zinc ion (Figure 6a1). This was confirmed from the bond distance between the active site zinc ion and a water molecule that moved from the exterior of the HDAC1 protein into the active site to replace the LLX and that maintained the zinc coordination (Figure 6a2). Initially the bond distance between them was  $\sim 10 \text{ \AA}$ , but over simulation, this bond distance started to drop as the water molecule moved toward the active site and finally fell to  $\sim 2 \text{ \AA}$  at around 50 ps, after which the distance was maintained around this range. This implied that the water transportation between the catalytic site and the exterior of the protein had important roles in the structure and function of these proteins.

Nevertheless, the backbone RMSD values for almost all the egress trajectories through channel A were between 0.7 and 1.0  $\text{\AA}$ , and this evidenced that the ligand release through this channel did not induce many conformational changes to these protein structures. Also, as this was a very short pathway with only 11  $\text{\AA}$  in length, the total expulsion times for the ligand in most of the structures did not exceed 150 ps.

**Characteristics of Channel B1.** Channel B1 in both HDAC1 and HDAC2 enzymes were similar in their structures and were composed of nonpolar amino acids and outlined by the aromatic residues. Channel B1 lied between the loop adjoining the eight-stranded  $\beta$ -sheets and the loop adjoining

Table 2. Pencil Sketch Showing the Ligand Expulsion through Channels A and B in HDAC2<sup>a</sup>

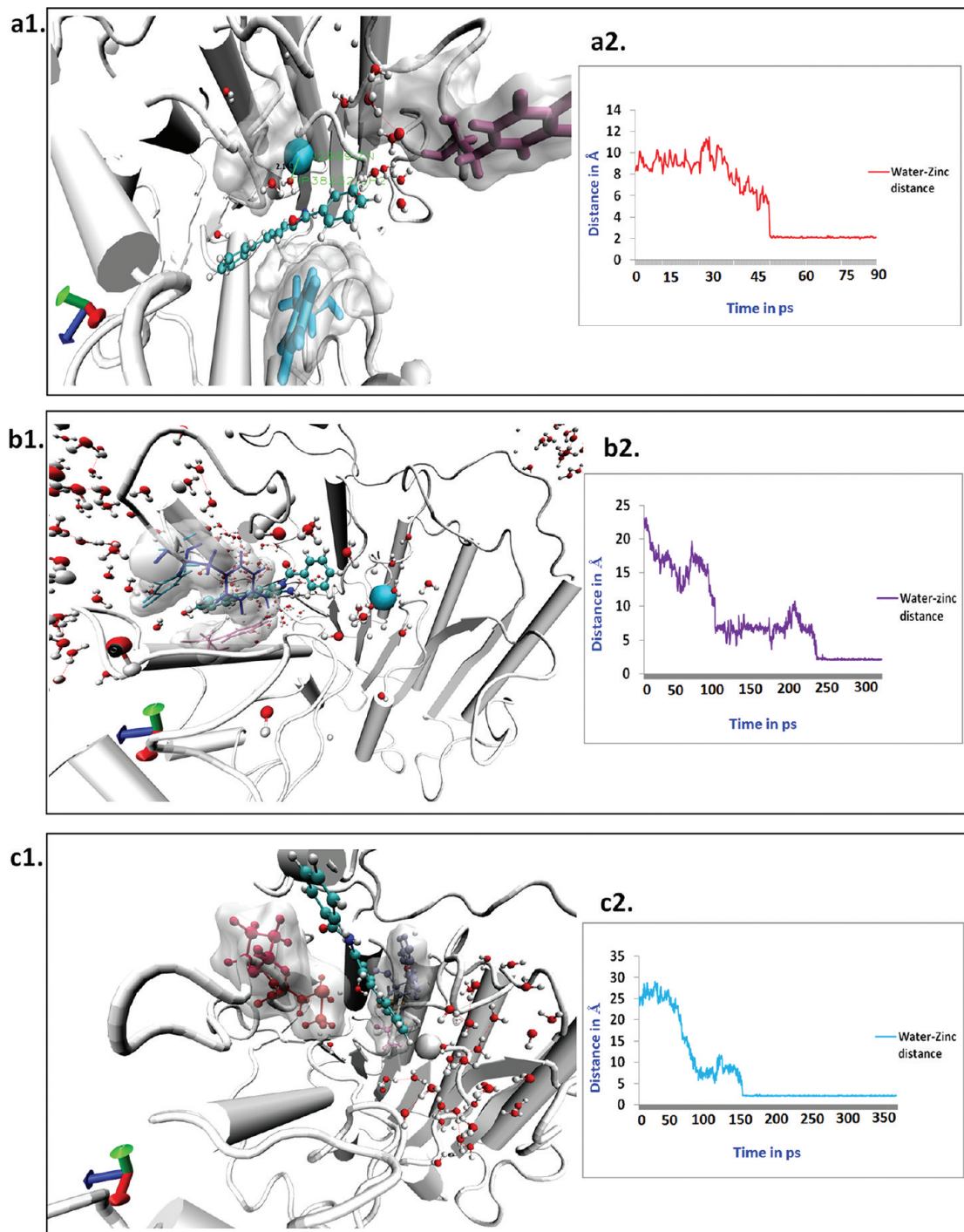
<sup>a</sup>(I.a) Initially, the Phe 155 residue remains closed with its dihedral towards 60°, thereby keeping the ligand into binding pocket. (I.b) Over simulation time, this Phe residue flips its side chain to almost 180° and -60°, therefore breaking the ligand contact and offering more space for its expulsion. (c) Finally, the ligand achieves its expulsion through the permanently opened channel A. (II.a) Originally, the phenyl rings of the three aromatic residues, Tyr 29 and Phe 114 (with the dihedral angle towards -60°) from one side and Tyr 27 (with a dihedral of 60°) on the other side, are closed together, thereby blocking the ligand egress channel. (b) Eventually, these three aromatic residues flipped their side chains (now, Tyr 29 and Phe 114 residues with the dihedral close to 60° and the Tyr27 close to -60°), thereby opening the pathway B for ligand exit. (c) Finally, after the ligand exit, these residues turned back to their actual positions. The conformations of the residues are given within parentheses: g<sup>-</sup>, gauche<sup>-</sup>; g<sup>+</sup>, gauche<sup>+</sup>; and t, trans.

the longer  $\alpha$ -helix, which temporarily opened to the exterior of the HDAC1 and HDAC2 (Figure 4b,e) proteins to communicate with the bulk solvent. Here, the exit event began when the ligand, with the implied force, broke its interactions with the zinc ion and the Phe 205/210 contacts. Identical to the mechanisms in channel A, the ligand exiting through channel B1 was also inside the cavity until it lost its strong hydrophobic contacts with Phe 150/155 and Phe 205/210 residues, after which it was able to wander inside the protein space. But, unlike channel A, the ligand through channel B1 did not exit immediately after crossing the Phe residues but had to wait for the temporary tunnel opening before continuing its egress travel (Figure 5b).

Three aromatic residues, including two tyrosine residues on one side (Tyr 22, Tyr 24 in HDAC1; Tyr 27, Tyr 29 in HDAC2) and one phenylalanine (Phe 109 in HDAC1; Phe 114 in HDAC2) on the opposite side, together served as the gate-keeping residues in channel B1. The side chains of the tyrosine residues tilted toward phenyl ring of the phenylalanine on the other side, thereby closing the gate on this protein channel. The ligand moved out to the bulk solvent by an aromatic gating mechanism that imitated the ‘unzip’ process by which the two loops moved backward clearing the egress route (Figure 5b and Table 2). The unzipping mechanism was aided by the exchange of water molecules between the protein and the bulk solvent (Figure 6b). The dihedral plots of the tyrosine residues involving in this gating mechanism revealed that these amino acids had skewed their side chains between the gauche<sup>-</sup> and trans conformers during the simulation (Table 3). For instance, in HDAC1, when the zipper was ‘on’, the Phe 109 was in

gauche<sup>+</sup> conformation, and the Tyr 22 and Tyr 24 remained in gauche<sup>-</sup> conformations. Conversely, when the zipper was ‘off’, these residues shifted to their respective opposite configurations (i.e., Phe 109 to gauche<sup>-</sup>; Tyr 22 and Tyr 24 into gauche<sup>+</sup>), thereby opening the gate for the ligand exit. The overall exit time through this channel was from 300 ps to 1 ns. Furthermore, the backbone RMSD values for all the egress trajectories of channel B1 were in the range of 1.5–3 Å. This confirmed that the ligand release through this pathway provoked larger structural changes in the proteins compared to channels A and B1. In addition, water exchange between the buried active site and the bulk solvent through channel B1 was also witnessed (Figure 6b1). Like in channel A, the zinc coordination in channel B1 was also maintained by a water molecule that traversed from the bulk solvent into the protein active site and replaced the ligand. The distance between the zinc ion and the water molecule that passed through the channel B1 into active site of HDAC1 was initially ~25 Å but later dropped to ~2 Å at around 230 ps, indicating that the water molecule had successfully coordinated with the zinc ion, upon the unbinding of the ligand from the active site zinc ion (Figure 6b2). Similar mechanism of water was also observed during the ligand egression through channel B1 in HDAC2 enzymes.

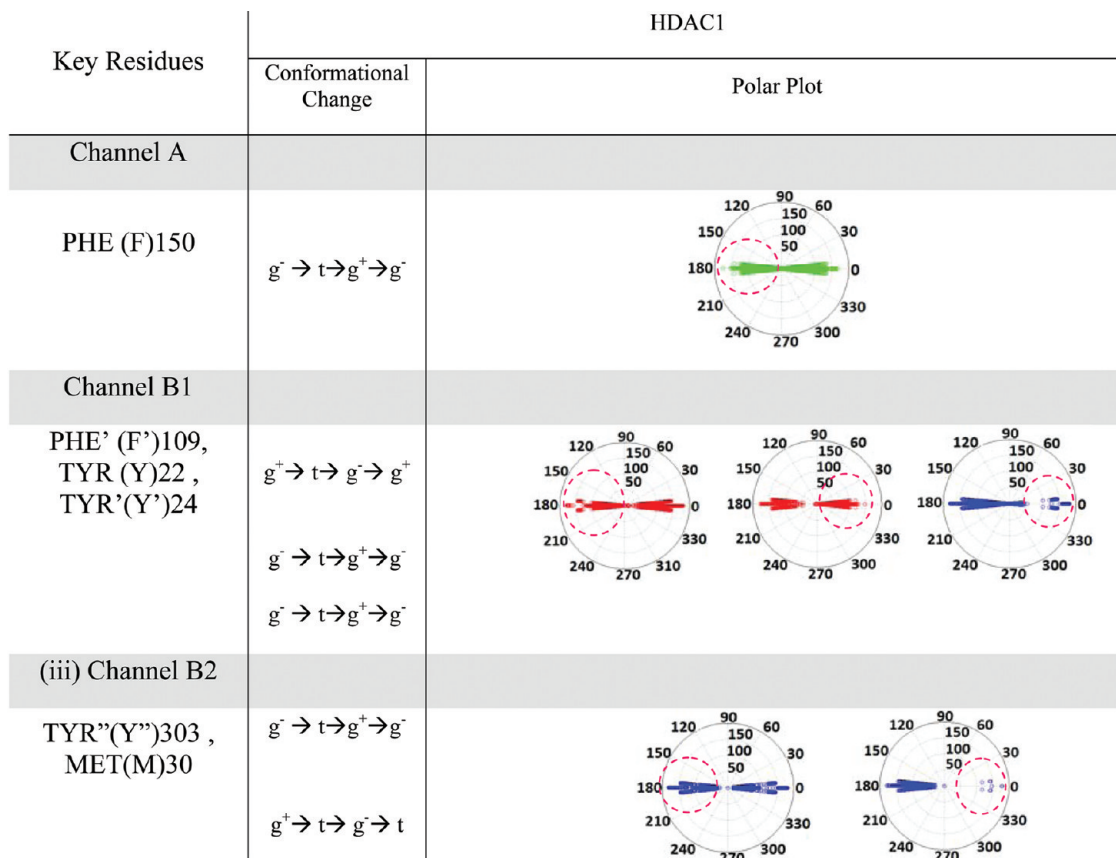
**Characteristics of Channel B2.** Channel B2, a subpathway from the channel B1, was unique to HDAC1 protein and was not identified in HDAC2. This channel of approximately 16 Å (region covering part of Channel B1 until the groove and the diverted channel, all together) was located between the linking loops of two parallel  $\beta$  sheets of the  $\beta$ - $\alpha$ - $\beta$  motifs and was



**Figure 6.** Role of water in zinc coordination. Water maintaining the zinc coordination after ligand starts expulsion along (a–c) channels A, B1, and B2.

perpendicular to the channel A (Figure 4c). The initial steps in exit mechanisms through channel B2 followed the same series as the other two pathways: where the ligand broke the contacts with the metal center, the two Phe residues and subsequently started moving toward the direction of channel B1 but then turned around 90° and started probing a new direction for exit to the bulk solvent through a new gateway. The two amino acids, Met 30 and Tyr 303, acted as the gateway residues for this channel. Here, the para hydroxyl group of the tyrosine made hydrogen bonding with the methionine and these residues changed their side chain orientations to keep this

temporary path clear for the ligand exit (Figure 5c and Table 2). Initially, the Tyr 303 was in gauche<sup>-</sup> configuration with a dihedral angle  $\sim 180^\circ$  and Met 30 at gauche<sup>-</sup> configuration with  $30^\circ$ . However, these residues changed to their opposite conformation, where Tyr 303 as gauche<sup>+</sup> and Met 30 as gauche<sup>-</sup>, thereby clearing this channel B2 for ligand exit (Figure 5c and Table 2). Upon ligand exit, these residues returned to their original state, thereby closing this transient tunnel. The RMSD value for all the egress trajectories through channel B2 was below 2.6 Å, and the expulsion time required to complete the egression was from 300 ps to 800 ps. This revealed that the

Table 3. Key Residues Table<sup>a</sup>

<sup>a</sup>Conformation changes of the key residues and their corresponding polar plots showing the dihedral shift in the residues during the RAMD simulations of HDAC1 enzyme.

Table 4. Characteristic Features of the Different Protein Channels in HDAC1 and HDAC2 Identified Through RAMD Simulations

Channels	Exit Direction	Length	Type	HDAC1			HDAC2		
				Key Residues	Average Egression Time in ps		Key Residues	Average Egression Time in ps	
					Min	Max		Min	Max
A	Zn	11 Å	Permanent	Phe150	100	150	Phe155	100	200
B1	Zn	~14 Å	Transient	Phe109, Tyr22, Tyr24	275	850	Phe114, Tyr27, Tyr29	600	750
B2	Zn	~16 Å	Transient	Tyr303, Met 30	380	670	N/A	N/A	N/A

target structure had undergone few changes upon ligand exit via this channel. This channel B2 was also used for the water exchange within the HDAC1 active site and the bulk solvent. The water molecules, as observed in the other channels, played significant roles in coordinating with the metal ion when the ligand began to escape the cavity (Figure 6c1 and c2).

## ■ DISCUSSION

In the efforts of exploring the HDAC protein channels, we have identified a number of interesting and significant observations on these HDAC structures, which are reported in Table 4.

**Phe 150/155: A Key Residue for HDAC Activity.** RAMD simulations recognized that the phenylalanine residue, which is located in the second sphere of the HDAC binding site, has a very significant role in the structures and functions of the HDAC enzymes. Our results show that the Phe residue in the second catalytic sphere, Phe 150 in HDAC1 and Phe 155 in HDAC2, not only helps in providing access to the ligand but also plays a significant role in positioning and holding the ligand within the active site through favorable hydrophobic interactions. This inference provides insights on the previous experimental study,<sup>12</sup> which strongly supports the importance of the Phe 150 aromatic residue in the enzymatic activity of HDAC1. Weerasinghe et al.<sup>12</sup> have conducted combined mutagenesis experiments on HDAC1, where they mutated Phe150 residues with several natural amino acids and tested the mutants using *in vitro* fluorescence assay.<sup>12</sup> They identified that substitution of Phe150 with alanine resulted in the reduced enzymatic activity. In consistent with these findings, our RAMD simulations revealed that, irrespective of the channel, the ligand release event in the HDAC1 and HDAC2 proteins was initiated only after breaking the strong hydrophobic interactions between the ligand and the Phe 150/155 residue in HDAC1/HDAC2, respectively. Hence, this aromatic residue is highly significant in the ligand exit mechanisms and is uniquely essential for preserving the biological functions of the HDAC1 and HDAC2 proteins.

**Gate-Keeping Aromatic Residues.** ‘Aromatic gating’ remains a common, yet an interesting, phenomenon through which the enzymes with buried catalytic centers control the motilities or accessibilities of several elements, including ligands and water molecules. Such interesting aromatic gating incidences were described in several other previous studies involving haloalkane dehalogenases,<sup>45,46</sup> cytochrome P450 2C9,<sup>78</sup> cytochrome P450 2A6,<sup>47</sup> hexameric insulin–phenol complexes, and acetylcholinesterase.<sup>79–81</sup> This study on HDAC enzymes also identifies a few specific aromatic residues that serve as gate keepers in the channels of these enzymes that control these tunnels and also the ligand unbinding events. As described above, the Phe 150/155 and Phe 205/210 residues are key entities that react to initiate ligand egression. However, there were also other residues recognized to be involved in the ligand release events. Two tyrosines (Tyr 22 and Tyr 24 in HDAC1; Tyr 27 and Tyr 29 in HDAC2) and one phenylalanine (Phe 109 in HDAC1; Phe 114 in HDAC2) residues together involved in a transient ‘zip-on/zip-off’ mechanism to allow ligand exit through channel B1 in the proteins. Additionally, Tyr 303, along with Met 30, is significant for the opening and closing of the channel B2 identified in the HDAC1 enzyme. Thus, the aromatic amino acids act as the gate keepers in the protein channels of the HDAC1 and HDAC2 enzymes, thereby involving in the various structural changes that take place within them. The entire list of amino

acid residues lining the channels A, B1 and B2 in HDAC1 and HDAC2 are presented in Table 1, Supporting Information. Hence, the proposed gate-keeping residues and the other amino acids lining the channels of these HDACs may be mutated to confirm their roles in the ligand egression processes and also the functionalities of the enzymes.

**Substrate–Product Release: A Hypothesis.** Previous docking-based simulation study<sup>33</sup> proposed that the 11 Å channel A has no favorable binding sites to suite the acetate product release occurring after the hydrolysis of the lysine substrate. Moreover, when the acetyl group is cleaved from the acetylated lysine, the protonated lysine residue stays engaged at the permanent channel A, blocking the pathway for product release. Hence, an alternate tunnel becomes inevitable for the product release events. The transient channels, B1 and B2, identified in this study, are close to the binding site and spacious enough to accommodate the product release event. Several previous studies have hypothesized that the product release could occur via channel B1. In addition to these hypotheses, we identified a unique channel B2 in the HDAC1, which followed the path along the channel B1 and later diverged into a new direction. We speculate that the product release events could also happen through this transient channel identified in this study. Our future work will be in this direction toward carrying out combined RAMD and SMD simulations of the substrate–product release from the HDAC enzymes and free energy profiling of the different pathways to identify the most favorable channels.

## ■ SUMMARY AND CONCLUSIONS

The release of the LLX ligand from the buried zinc-dependent active sites of the recently solved X-ray crystal structure of the HDAC2 and the computationally modeled HDAC1 enzymes were simulated using the combined RAMD and classical MD simulations. In this study, we investigated the known pathways (channels A and B1) and also identified additional pathway (channel B2) for ligand release and water exchange in HDAC1 and HDAC2 enzymes. The key gate-keeping residues that controlled the dynamic features of the channels were identified, and mutagenesis experiments on these gate-keeping aromatic and other amino acid residues would be desirable to confirm their roles in the functional properties of the HDAC1 and HDAC2 enzymes. Such information would be useful to develop a more mechanistic understanding of the HDAC enzymes.

## ■ ASSOCIATED CONTENT

### S Supporting Information

Sequence alignment of template and the target; superimposed structures of the modeled protein and the template; Ramachandran plot of the modeled structure; open and close channel conformations from HDAC2 MD simulation; water exchange during MD simulations; residues lining the HDAC channels; and simulation parameters. This information is available free of charge via the Internet at <http://pubs.acs.org>.

## ■ AUTHOR INFORMATION

### Corresponding Author

\*E-mail: phoebe.chen@latrobe.edu.au. Telephone: +61 3 94792598.

### Notes

The authors declare no competing financial interest.

## ■ REFERENCES

- (1) Levy, D.; Gozani, O. Decoding Chromatin Goes High Tech. *Cell* **2010**, *142*, 844–846.
- (2) Hodawadekar, S. C.; Marmorstein, R. Chemistry of acetyl transfer by histone modifying enzymes: structure, mechanism and implications for effector design. *Oncogene* **2007**, *26*, 5528–5540.
- (3) Lee, J.-S.; Smith, E.; Shilatifard, A. The Language of Histone Crosstalk. *Cell* **2010**, *142*, 682–685.
- (4) Vannini, A.; Volpari, C.; Filocamo, G.; Casavola, E. C.; Brunetti, M.; Renzoni, D.; Chakravarty, P.; Paolini, C.; De Francesco, R.; Gallinari, P.; Steinkühler, C.; Di Marco, S. Crystal structure of a eukaryotic zinc-dependent histone deacetylase, human HDAC8, complexed with a hydroxamic acid inhibitor. *Proc. Natl. Acad. Sci. U.S.A.* **2004**, *101*, 15064–15069.
- (5) Simonsson, M.; Heldin, C.-H.; Ericsson, J.; Gronroos, E. The Balance between Acetylation and Deacetylation Controls Smad7 Stability. *J. Biol. Chem.* **2005**, *280*, 21797–21803.
- (6) Grunstein, M. Histone acetylation in chromatin structure and transcription. *Nature* **1997**, *389*, 349–352.
- (7) Grozinger, C. M.; Schreiber, S. L. Deacetylase Enzymes: Biological Functions and the Use of Small-Molecule Inhibitors. *Chem. Biol.* **2002**, *9*, 3–16.
- (8) Mottet, D.; Castronovo, V. Histone deacetylases: target enzymes for cancer therapy. *Clin. Exp. Metastasis* **2008**, *25*, 183–189.
- (9) Kim, I. A.; Shin, J. H.; Kim, I. H.; Kim, J. H.; Kim, J. S.; Wu, H. G.; Chie, E. K.; Ha, S. W.; Park, C. I.; Kao, G. D. Histone Deacetylase Inhibitors-Mediated Radiosensitization of Human Cancer Cells: Class Differences and the Potential Influence of p53. *Clin. Cancer Res.* **2006**, *12*, 940–949.
- (10) Wu, R.; Wang, S.; Zhou, N.; Cao, Z.; Zhang, Y. A Proton-Shuttle Reaction Mechanism for Histone Deacetylase 8 and the Catalytic Role of Metal Ions. *J. Am. Chem. Soc.* **2010**, *132*, 9471–9479.
- (11) Bradner, J. E.; West, N.; Grachan, M. L.; Greenberg, E. F.; Haggarty, S. J.; Warnow, T.; Mazitschek, R. Chemical phylogenetics of histone deacetylases. *Nat. Chem. Biol.* **2010**, *6*, 238–243.
- (12) Weerasinghe, S. V. W.; Estiu, G.; Wiest, O.; Pflum, M. K. H. Residues in the 11 Å Channel of Histone Deacetylase 1 Promote Catalytic Activity: Implications for Designing Isoform-Selective Histone Deacetylase Inhibitors. *J. Med. Chem.* **2008**, *51*, 5542–5551.
- (13) Tang, H.; Wang, X. S.; Huang, X.-P.; Roth, B. L.; Butler, K. V.; Kozikowski, A. P.; Jung, M.; Tropsha, A. Novel Inhibitors of Human Histone Deacetylase (HDAC) Identified by QSAR Modeling of Known Inhibitors, Virtual Screening, and Experimental Validation. *J. Chem. Inf. Model.* **2009**, *49*, 461–476.
- (14) de Ruijter, A.; van Gennip, A.; Caron, H.; Kemp, S.; van Kuilenburg, A. Histone deacetylases (HDACs): characterization of the classical HDAC family. *Biochem. J.* **2003**, *370*, 737–749.
- (15) Ropero, S.; Esteller, M. The role of histone deacetylases (HDACs) in human cancer. *Mol. Oncol.* **2007**, *1*, 19–25.
- (16) Frolov, M. V.; Dyson, N. J. Molecular mechanisms of E2F-dependent activation and pRB-mediated repression. *J. Cell Sci.* **2004**, *117*, 2173–2181.
- (17) Consortium, T. U. Ongoing and future developments at the Universal Protein Resource. *Nucleic Acids Res.* **2011**, *39*, D214–D219.
- (18) Ropero, S.; Fraga, M. F.; Ballestar, E.; Hamelin, R.; Yamamoto, H.; Boix-Chornet, M.; Caballero, R.; Alaminos, M.; Setien, F.; Paz, M. F.; Herranz, M.; Palacios, J.; Arango, D.; Orntoft, T. F.; Aaltonen, L. A.; Schwartz, S.; Esteller, M. A truncating mutation of HDAC2 in human cancers confers resistance to histone deacetylase inhibition. *Nat. Genet.* **2006**, *38*, 566–569.
- (19) Huang, B.; Laban, M.; Leung, C.; Lee, L.; Lee, C.; Salto-Tellez, M.; Raju, G.; Hooi, S. Inhibition of histone deacetylase 2 increases apoptosis and p21Cip1/WAF1 expression, independent of histone deacetylase 1. *Cell Death Differ.* **2005**, *12*, 395–404.
- (20) Zhu, P.; Martin, E.; Mengwasser, J.; Schlag, P.; Janssen, K.-P.; Göttlicher, M. Induction of HDAC2 expression upon loss of APC in colorectal tumorigenesis. *Cancer Cell* **2004**, *5*, 455–463.
- (21) Schapira, M. Structural Biology of Human Metal-Dependent Histone Deacetylases. In *Histone Deacetylases: the Biology and Clinical Implication*. Yao, T.-P.; Seto, E., Eds.; Springer: Berlin, Heidelberg, Germany, 2011; pp 206, 225–240.
- (22) de Ruijter, A. J. M.; van Gennip, A. H.; Caron, H. N.; Kemp, S.; van Kuilenburg, A. B. P. Histone deacetylases (HDACs): characterization of the classical HDAC family. *Biochem. J.* **2003**, *370*, 737–749.
- (23) Finnin, M. S.; Dongian, J. R.; Cohen, A.; Richon, V. M.; Rifkind, R. A.; Marks, P. A.; Breslow, R.; Pavletich, N. P. Structures of a histone deacetylase homologue bound to the TSA and SAHA inhibitors. *Nature* **1999**, *401*, 188–193.
- (24) Liu, T.; Kuljaca, S.; Tee, A.; Marshall, G. M. Histone deacetylase inhibitors: Multifunctional anticancer agents. *Cancer Treat. Rev.* **2006**, *32*, 157–165.
- (25) Merzvinskyte, R.; Treigyte, G.; Savickiene, J.; Magnusson, K.-E.; Navakauskiene, R. Effects of Histone Deacetylase Inhibitors, Sodium Phenyl Butyrate and Vitamin B3, in Combination with Retinoic Acid on Granulocytic Differentiation of Human Promyelocytic Leukemia HL-60 Cells. *Ann. N. Y. Acad. Sci.* **2006**, *1091*, 356–367.
- (26) Dokmanovic, M.; Marks, P. A. Prospects: Histone deacetylase inhibitors. *J. Cell. Biochem.* **2005**, *96*, 293–304.
- (27) Andrianov, V.; Gailite, V.; Lola, D.; Loza, E.; Semenikhina, V.; Kalvinsh, I.; Finn, P.; Petersen, K. D.; Ritchie, J. W. A.; Khan, N.; Tumber, A.; Collins, L. S.; Vadlamudi, S. M.; Björkling, F.; Sehested, M. Novel amide derivatives as inhibitors of histone deacetylase: Design, synthesis and SAR. *Eur. J. Med. Chem.* **2009**, *44*, 1067–1085.
- (28) Wu, R.; Lu, Z.; Cao, Z.; Zhang, Y. Zinc Chelation with Hydroxamate in Histone Deacetylases Modulated by Water Access to the Linker Binding Channel. *J. Am. Chem. Soc.* **2011**, *133*, 6110–6113.
- (29) Bieliauskas, A. V.; Pflum, M. K. H. Isoform-selective histone deacetylase inhibitors. *Chem. Soc. Rev.* **2008**, *37*, 1402–1413.
- (30) Ortore, G.; Colo, F. D.; Martinelli, A. Docking of Hydroxamic Acids into HDAC1 and HDAC8: A Rationalization of Activity Trends and Selectivities. *J. Chem. Inf. Model.* **2009**, *49*, 2774–2785.
- (31) Zhou, H.-X.; Wlodek, S. T.; McCammon, J. A. Conformation gating as a mechanism for enzyme specificity. *Proc. Natl. Acad. Sci. U.S.A.* **1998**, *95*, 9280–9283.
- (32) Estiu, G.; Greenberg, E.; Harrison, C. B.; Kwiatkowski, N. P.; Mazitschek, R.; Bradner, J. E.; Wiest, O. Structural Origin of Selectivity in Class II-Selective Histone Deacetylase Inhibitors. *J. Med. Chem.* **2008**, *51*, 2898–2906.
- (33) Wang, D.-F.; Wiest, O.; Helquist, P.; Lan-Harget, H.-Y.; Wiech, N. L. On the Function of the 14 Å Long Internal Cavity of Histone Deacetylase-Like Protein: Implications for the Design of Histone Deacetylase Inhibitors. *J. Med. Chem.* **2004**, *47*, 3409–3417.
- (34) Wang, D. Computational Studies on the Histone Deacetylases and the Design of Selective Histone Deacetylase Inhibitors. *Curr. Top. Med. Chem.* **2009**, *9*, 241–256.
- (35) Bressi, J. C.; Jennings, A. J.; Skene, R.; Wu, Y.; Melkus, R.; Jong, R. D.; O'Connell, S.; Grimshaw, C. E.; Navre, M.; Gangloff, A. R. Exploration of the HDAC2 foot pocket: Synthesis and SAR of substituted N-(2-aminophenyl)benzamides. *Bioorg. Med. Chem. Lett.* **2010**, *20*, 3142–3145.
- (36) Haider, S.; Joseph, C. G.; Neidle, S.; Fierke, C. A.; Fuchter, M. J. On the function of the internal cavity of histone deacetylase protein 8: R37 is a crucial residue for catalysis. *Bioorg. Med. Chem. Lett.* **2011**, *21*, 2129–2132.
- (37) Wang, H.; Dymock, B. W. New patented histone deacetylase inhibitors. *Expert Opin. Ther. Pat.* **2009**, *19*, 1727–1757.
- (38) Whitehead, L.; Dobler, M. R.; Radetich, B.; Zhu, Y.; Atadja, P. W.; Claiborne, T.; Grob, J. E.; McRiner, A.; Pancost, M. R.; Patnaik, A.; Shao, W.; Shultz, M.; Tichkule, R.; Tommasi, R. A.; Vash, B.; Wang, P.; Stams, T. Human HDAC isoform selectivity achieved via exploitation of the acetate release channel with structurally unique small molecule inhibitors. *Bioorg. Med. Chem.* **2011**, *19*, 4626–4634.
- (39) Lin, T.-L.; Song, G. Efficient mapping of ligand migration channel networks in dynamic proteins. *Proteins: Struct., Funct., Bioinf.* **2011**, *79*, 2475–2490.
- (40) Laio, A.; Gervasio, F. L. Metadynamics: a method to simulate rare events and reconstruct the free energy in biophysics, chemistry and material science. *Rep. Prog. Phys.* **2008**, *71*, 126601.

- (41) Liao, A.; Parrinello, M. Escaping free-energy minima. *Proc. Natl. Acad. Sci. U.S.A.* **2002**, *99*, 12562–12566.
- (42) Colizzi, F.; Perozzo, R.; Scapozza, L.; Recanatini, M.; Cavalli, A. Single-Molecule Pulling Simulations Can Discern Active from Inactive Enzyme Inhibitors. *J. Am. Chem. Soc.* **2010**, *132*, 7361–7371.
- (43) Park, S.; Schulten, K. Calculating potentials of mean force from steered molecular dynamics simulations. *J. Chem. Phys.* **2004**, *120*, 5946–5961.
- (44) Lüdemann, S. K.; Louannas, V.; Wade, R. C. How do substrates enter and products exit the buried active site of cytochrome P450cam? I. Random expulsion molecular dynamics investigation of ligand access channels and mechanisms. *J. Mol. Biol.* **2000**, *303*, 797–811.
- (45) Klvana, M.; Pavlova, M.; Koudelakova, T.; Chaloupkova, R.; Dvorak, P.; Prokop, Z.; Stsiapanava, A.; Kuty, M.; Kuta-Smatanova, I.; Dohnalek, J.; Kulhanek, P.; Wade, R. C.; Damborsky, J. Pathways and Mechanisms for Product Release in the Engineered Haloalkane Dehalogenases Explored Using Classical and Random Acceleration Molecular Dynamics Simulations. *J. Mol. Biol.* **2009**, *392*, 1339–1356.
- (46) Pavlova, M.; Klvana, M.; Prokop, Z.; Chaloupkova, R.; Banas, P.; Otyepka, M.; Wade, R. C.; Tsuda, M.; Nagata, Y.; Damborsky, J. Redesigning dehalogenase access tunnels as a strategy for degrading an anthropogenic substrate. *Nat. Chem. Biol.* **2009**, *5*, 727–733.
- (47) Li, W.; Shen, J.; Liu, G.; Tang, Y.; Hoshino, T. Exploring coumarin egress channels in human cytochrome p450 2a6 by random acceleration and steered molecular dynamics simulations. *Proteins: Struct., Funct., Bioinf.* **2011**, *79*, 271–281.
- (48) Long, D.; Mu, Y.; Yang, D. Molecular Dynamics Simulation of Ligand Dissociation from Liver Fatty Acid Binding Protein. *PLoS One* **2009**, *4*, e6081.
- (49) Wang, T.; Duan, Y. Ligand Entry and Exit Pathways in the  $\beta 2$ -Adrenergic Receptor. *J. Mol. Biol.* **2009**, *392*, 1102–1115.
- (50) Wang, T.; Duan, Y. Retinal release from opsin in molecular dynamics simulations. *J. Mol. Recognit.* **2011**, *24*, 350–358.
- (51) Gaulton, A.; Bellis, L. J.; Bento, A. P.; Chambers, J.; Davies, M.; Hersey, A.; Light, Y.; McGlinchey, S.; Michalovich, D.; Al-Lazikani, B.; Overington, J. P. ChEMBL: a large-scale bioactivity database for drug discovery. *Nucleic Acids Res.* **2012**, *40*, D1100–D1107.
- (52) Fréchette, S.; Leit, S.; Woo, S. H.; Lapointe, G.; Jeannotte, G.; Moradei, O.; Paquin, I.; Bouchain, G.; Raeppe, S.; Gaudette, F.; Zhou, N.; Vaisburg, A.; Fournel, M.; Yan, P. T.; Trachy-Bourget, M.-C.; Kalita, A.; Robert, M.-F.; Lu, A.; Rahil, J.; Robert MacLeod, A.; Besterman, J. M.; Li, Z.; Delorme, D. 4-(Heteroarylaminomethyl)-N-(2-aminophenyl)-benzamides and their analogs as a novel class of histone deacetylase inhibitors. *Bioorg. Med. Chem. Lett.* **2008**, *18*, 1502–1506.
- (53) Methot, J. L.; Chakravarty, P. K.; Chenard, M.; Close, J.; Cruz, J. C.; Dahlberg, W. K.; Fleming, J.; Hamblett, C. L.; Hamill, J. E.; Harrington, P.; Harsch, A.; Heidebrecht, R.; Hughes, B.; Jung, J.; Kenific, C. M.; Kral, A. M.; Meinke, P. T.; Middleton, R. E.; Ozerova, N.; Sloman, D. L.; Stanton, M. G.; Szewczak, A. A.; Tyagarajan, S.; Witter, D. J.; Paul Sechrist, J.; Miller, T. A. Exploration of the internal cavity of histone deacetylase (HDAC) with selective HDAC1/HDAC2 inhibitors (SHI-1:2). *Bioorg. Med. Chem. Lett.* **2008**, *18*, 973–978.
- (54) Moradei, O.; Leit, S.; Zhou, N.; Fréchette, S.; Paquin, I.; Raeppe, S.; Gaudette, F.; Bouchain, G.; Woo, S. H.; Vaisburg, A.; Fournel, M.; Kalita, A.; Lu, A.; Trachy-Bourget, M.-C.; Yan, P. T.; Liu, J.; Li, Z.; Rahil, J.; MacLeod, A. R.; Besterman, J. M.; Delorme, D. Substituted N-(2-aminophenyl)-benzamides, (E)-N-(2-aminophenyl)-acrylamides and their analogues: Novel classes of histone deacetylase inhibitors. *Bioorg. Med. Chem. Lett.* **2006**, *16*, 4048–4052.
- (55) Lin, Y.-C.; Lin, J.-H.; Chou, C.-W.; Chang, Y.-F.; Yeh, S.-H.; Chen, C.-C. Statins Increase p21 through Inhibition of Histone Deacetylase Activity and Release of Promoter-Associated HDAC1/2. *Cancer Res.* **2008**, *68*, 2375–2383.
- (56) Stote, R. H.; Karplus, M. Zinc binding in proteins and solution: A simple but accurate nonbonded representation. *Proteins: Struct., Funct., Bioinf.* **1995**, *23*, 12–31.
- (57) Kaminski, G. A.; Friesner, R. A.; Tirado-Rives, J.; Jorgensen, W. L. Evaluation and Reparametrization of the OPLS-AA Force Field for Proteins via Comparison with Accurate Quantum Chemical Calculations on Peptides<sup>†</sup>. *J. Phys. Chem. B* **2001**, *105*, 6474–6487.
- (58) Jacobson, M. P.; Friesner, R. A.; Xiang, Z.; Honig, B. On the Role of the Crystal Environment in Determining Protein Side-chain Conformations. *J. Mol. Biol.* **2002**, *320*, 597–608.
- (59) Jacobson, M. P.; Pincus, D. L.; Rapp, C. S.; Day, T. J. F.; Honig, B.; Shaw, D. E.; Friesner, R. A. A hierarchical approach to all-atom protein loop prediction. *Proteins: Struct., Funct., Bioinf.* **2004**, *55*, 351–367.
- (60) Mobley, D. L.; Dill, K. A. Binding of Small-Molecule Ligands to Proteins: What You See Is Not Always What You Get. *Structure (London, U.K.)* **2009**, *17*, 489–498.
- (61) Helms, V. Protein Dynamics Tightly Connected to the Dynamics of Surrounding and Internal Water Molecules. *ChemPhysChem* **2007**, *8*, 23–33.
- (62) Karin Schleinkofer, S.; Winn, P. J.; Lüdemann, S. K.; Wade, R. C. Do mammalian cytochrome P450s show multiple ligand access pathways and ligand channelling? *EMBO Rep.* **2005**, *6*, 584–589.
- (63) Tomita, A.; Sato, T.; Ichiyanagi, K.; Nozawa, S.; Ichikawa, H.; Chollet, M.; Kawai, F.; Park, S.-Y.; Tsuduki, T.; Yamato, T.; Koshihara, S.-y.; Adachi, S.-i. Visualizing breathing motion of internal cavities in concert with ligand migration in myoglobin. *Proc. Natl. Acad. Sci. U.S.A.* **2009**, *106*, 2612–2616.
- (64) Winn, P. J.; Lüdemann, S. K.; Gauges, R.; Louannas, V. R.; Wade, R. C. Comparison of the dynamics of substrate access channels in three cytochrome P450s reveals different opening mechanisms and a novel functional role for a buried arginine. *Proc. Natl. Acad. Sci. U.S.A.* **2002**, *99*, 5361–5366.
- (65) Brooks, B. R.; Bruccoleri, R. E.; Olafson, B. D.; States, D. J.; Swaminathan, S.; Karplus, M. CHARMM: A program for macromolecular energy, minimization, and dynamics calculations. *J. Comput. Chem.* **1983**, *4*, 187–217.
- (66) Kalé, L.; Skeel, R.; Bhandarkar, M.; Brunner, R.; Gursoy, A.; Krawetz, N.; Phillips, J.; Shinozaki, A.; Varadarajan, K.; Schulten, K. NAMD2: Greater Scalability for Parallel Molecular Dynamics. *J. Comput. Phys.* **1999**, *151*, 283–312.
- (67) Zoete, V.; Cuendet, M. A.; Grosdidier, A.; Michelin, O. SwissParam: A fast force field generation tool for small organic molecules. *J. Comput. Chem.* **2011**, *32*, 2359–2368.
- (68) Halgren, T. A. Merck molecular force field. I. Basis, form, scope, parameterization, and performance of MMFF94. *J. Comput. Chem.* **1996**, *17*, 490–519.
- (69) Kawata, M.; Nagashima, U. Particle mesh Ewald method for three-dimensional systems with two-dimensional periodicity. *Chem. Phys. Lett.* **2001**, *340*, 165–172.
- (70) Feller, S. E.; Zhang, Y.; Pastor, R. W.; Brooks, B. R. Constant pressure molecular dynamics simulation: The Langevin piston method. *J. Chem. Phys.* **1995**, *103*, 4613–4621.
- (71) Schmidt, A.; Lamzin, V. From atoms to proteins. *Cell. Mol. Life Sci.* **2007**, *64*, 1959–1969.
- (72) Cojocaru, V.; Winn, P. J.; Wade, R. C. The ins and outs of cytochrome P450s. *Biochim. Biophys. Acta, Gen. Subj.* **2007**, *1770*, 390–401.
- (73) Vashisth, H.; Abrams, C. F. Ligand Escape Pathways and (Un)Binding Free Energy Calculations for the Hexameric Insulin-Phenol Complex. *Biophys. J.* **2008**, *95*, 4193–4204.
- (74) Wang, T.; Duan, Y. Chromophore Channeling in the G-Protein Coupled Receptor Rhodopsin. *J. Am. Chem. Soc.* **2007**, *129*, 6970–6971.
- (75) Wang, T.; Duan, Y. Ligand Entry and Exit Pathways in the [beta]2-Adrenergic Receptor. *J. Mol. Biol.* **2009**, *392*, 1102–1115.
- (76) MATLAB, version 7.10.0 (R2010a); The MathWorks Inc.: NSW, Australia, 2010.
- (77) Amemiya, T.; Koike, R.; Kidera, A.; Ota, M. PSCDB: a database for protein structural change upon ligand binding. *Nucleic Acids Res.* **2012**, *40*, D554–D558.
- (78) Cojocaru, V.; Balali-Mood, K.; Sansom, M. S. P.; Wade, R. C. Structure and Dynamics of the Membrane-Bound Cytochrome P450 2C9. *PLoS Comput. Biol.* **2011**, *7*, e1002152.

- (79) Bui, J. M.; Henchman, R. H.; McCammon, J. A. The Dynamics of Ligand Barrier Crossing inside the Acetylcholinesterase Gorge. *Biophys. J.* **2003**, *85*, 2267–2272.
- (80) Kovach, I. M.; Qian, N.; Bencsura, A. Efficient product clearance through exit channels in substrate hydrolysis by acetylcholinesterase. *FEBS Lett.* **1994**, *349*, 60–64.
- (81) Ripoll, D. R.; Faerman, C. H.; Axelsen, P. H.; Silman, I.; Sussman, J. L. An electrostatic mechanism for substrate guidance down the aromatic gorge of acetylcholinesterase. *Proc. Natl. Acad. Sci. U.S.A.* **1993**, *90*, 5128–5132.